

Low-dimensional approach to pair production in an oscillating electric field: Application to bandgap graphene layers

I. Akal,^{*} R. Egger, C. Müller, and S. Villalba-Chávez[†]*Institut für Theoretische Physik, Heinrich-Heine-Universität Düsseldorf,**Universitätsstr. 1, 40225 Düsseldorf, Germany*

(Received 26 February 2016; published 24 June 2016)

The production of particle-antiparticle pairs from the quantum field theoretic ground state in the presence of an external electric field is studied. Starting with the quantum-kinetic Boltzmann-Vlasov equation in four-dimensional spacetime, we obtain the corresponding equations in lower dimensionalities by way of spatial compactification. Our outcomes in $2 + 1$ dimensions are applied to bandgap graphene layers, where the charge carriers have the particular property of behaving like light massive Dirac fermions. We calculate the single-particle distribution function for the case of an electric field oscillating in time and show that the creation of particle-hole pairs in this condensed matter system closely resembles electron-positron pair production by the Schwinger effect.

DOI: 10.1103/PhysRevD.93.116006

I. INTRODUCTION

Attaining the vacuum instability in a strong, macroscopically extended electromagnetic field through spontaneous creation of electron-positron pairs represents a major incentive for quantum electrodynamics (QED) and various branches of high-energy physics. For the case of a static electric field, the corresponding Schwinger rate of pair production (PP) has the form $\dot{\mathcal{N}} \sim \exp(-\pi E_c/E)$ [1–3], where E is the applied field and $E_c = m^2 c^3 / (|e| \hbar)$ the critical field of QED.¹ Due to its nonanalytic field dependence, the Schwinger effect exhibits a manifestly nonperturbative character. Its experimental observation, while being highly desirable, has been prevented until now by the huge value of $E_c \sim 10^{16}$ V/cm which is not accessible in the laboratory yet. It would not only verify a central prediction of QED, but also have implications for various other phenomena which share its principal features [4–7].

Substantial efforts are being made to bring the Schwinger effect into experimental reach. The next generation of high-intensity laser facilities currently under construction is expected to reach peak field intensities on the order of $\sim 10^{25}$ W/cm² [8,9]. The corresponding electric fields, having micrometer extensions and femtosecond durations, reach the percent level of the critical field E_c . To further increase the chance for an experimental realization of Schwinger PP, theoreticians have proposed to superimpose multiple laser beams [10], exploit the Lorentz boost inherent to relativistic particle-laser beam collisions

[11–13], or enhance the rate by the aid of an assisting high-frequency (photon) field [14–20].

While these sorts of facilitated Schwinger PP are very promising, they do not constitute the only way of probing the vacuum instability. Alternatively, one may follow a complementary route by inspecting physical environments where analogues of the Schwinger effect arise whose detection might be easier. Since its recent discovery, graphene [21–26] has become an ideal candidate for such a purpose. Fermionic quasiparticles close to one of the two K_{\pm} points in this two-dimensional monolayer of carbon atoms behave like relativistic particles [27]. They feature a dispersion relation like Dirac fermions, with the speed of light c being replaced by the Fermi velocity $v_f \approx c/300$, and the eigenstates have a Dirac spinor structure in sublattice space. As a consequence, fundamental phenomena of relativistic quantum physics find their low-energy counterpart in graphene, such as Klein tunneling [28], Coulomb supercriticality [25], many-body renormalization effects [26], or universal scaling phenomena [29].

Also, the analogue of Schwinger PP, i.e., field-induced creation of particle-hole pairs via low-energy electronic excitations from the valence to conduction band in graphene, has been studied theoretically. The process was examined by methods of $2 + 1$ -dimensional QED in a constant electric background [30],² a Sauter-like field [36], and an electric field oscillating in time [37,38]. The lack of an energy gap at the K_{\pm} points in graphene implies, however, that the charge carriers behave like massless Dirac fermions. This property prevents the existence of a critical field in graphene and, thus, the exponential

^{*}Present address: Theory Group, Deutsches Elektronen-Synchrotron DESY, Notkestr. 85, 22603 Hamburg, Germany.

[†]selym@tp1.uni-duesseldorf.de

¹Here and henceforth m and $|e|$ are the electron mass and its absolute charge, respectively. The speed of light in vacuum and the Planck constant are denoted by c and \hbar , respectively.

²In this background field, various related effects that might provide experimental signatures of the production of electron-hole pairs have been investigated [31–35].

suppression of the production rate that represents a main characteristic of the original Schwinger effect.

There are various techniques to induce a bandgap $\Delta\epsilon$ in graphene, e.g., by epitaxial growth on suitable substrates [39,40], elastic strain [26], or Rashba spin splittings on magnetic substrates [41]. Then a nonzero mass $m = \Delta\epsilon/(2v_f^2)$ is associated with the charge carriers whose high mobility still resembles the one of relativistic particles as long as their momenta lie below $\sim 3 \text{ eV}/v_f$ [24]. In this situation, the phenomenology of the field-induced particle-hole production process can be expected to show characteristics much closer to the electron-positron PP in QED. Such an analogy offers an ideal opportunity of getting valuable insights about the original Schwinger mechanism in an experimentally accessible low-energy domain. This is the motivation for the present study.

In this paper, we calculate the production of pairs of massive Dirac particles from the quantum field theoretic ground state in an external electric field. Starting from the well-known QED description of the process in $3+1$ dimensions, we develop a formalism in reduced dimensionality that is applicable to bandgap graphene layers. Analytical results for the production rate in a constant electric field (CEF) are obtained. For an electric field oscillating in time, the production rate and the momentum distribution of created particles are examined by numerical calculations. We demonstrate that—similar to PP in the unstable QED vacuum—the production of electron-hole pairs in a vicinity of the Dirac points in graphene layers is governed by a kinetic equation characterized by a non-Markovian nature and describe suitable field parameters for experimental observation of the effect.

Our paper is organized as follows. In Sec. II we describe some basic features of the PP process in an external electric field in $3+1$ -dimensional QED. Afterwards, by compactifying spatial dimensions, the quantum-kinetic Boltzmann-Vlasov equations in $2+1$ and $1+1$ dimensions are derived. The outcomes of this analyses are first applied to the case of a constant external electric field, where agreement with previous studies is found. This part is followed by a subsection which exposes the details necessary for applying the kinetic equation in $2+1$ dimensions to graphene layers. The numerical results are presented in Sec. III for the particular situation in which the electric field oscillates in time. We discuss the resonant effects and Rabi-like oscillations which arise in the single-particle distribution function. The density of pairs yielded is also investigated. Further comments and remarks are given in the conclusion.

II. QUANTUM-KINETIC APPROACH

A. General remarks in $3+1$ dimensions

First, we investigate the production of pairs in a field as can be conceived from laser waves. However, its

description represents a major task from both analytic and numeric viewpoints. Difficulties, introduced by the unavoidably complicated nature of such a wave, are frequently simplified for the sake of having a concise analytical description of the production process.³ A first step in this direction is taken by considering an electric-like background which can be obtained—to a good approximation—through a head-on collision of two linearly polarized laser pulses with equal intensities, frequencies and polarization directions. The field which results from this procedure is a spatially inhomogeneous standing electromagnetic wave depending on the temporal coordinate. However, for the numeric treatment, the dependence on the space coordinates still constitutes an important issue which is frequently avoided, although there exist already some first results including their effects [44,45]. Because of this, most of the studies developed in this research area consider the simplest model in which the background is a homogeneously distributed electric field oscillating in time [46–52].

There exist various theoretical approaches for describing the spontaneous production of electron-positron pairs in an external electromagnetic field. Many of them rely on the theoretical framework of QED in unstable vacuum [42]. In the case of a spatially homogeneous but time-dependent electric field $\mathbf{E}(t) = (0, E(t), 0)$,⁴ such a framework allows us to undertake the problem either through the S-matrix formalism [36,47–51,54,55] or from the transport theory point of view [19,56–64]. Both formulations are equivalent and complement each other. In this paper, we adopt the latter description which underlines the nonequilibrium nature of the PP. In this context, its investigation is carried out in terms of the distribution function $W(\mathbf{p}, t)$ of electrons and positrons to which the degrees of freedom in the external field are relaxed at asymptotically large times [$t \rightarrow \pm\infty$], i.e., when the electric field is switched off $\mathbf{E}(\pm\infty) \rightarrow 0$. The time evolution of this quantity is dictated by a quantum-kinetic equation involving a pronounced non-Markovian feature,⁵

$$\dot{W}(\mathbf{p}, t) = \frac{eE(t)\epsilon_{\perp}c}{w_p^2(t)} \int_{-\infty}^t dt' \frac{eE(t')\epsilon_{\perp}c}{w_p^2(t')} [1 - W(\mathbf{p}, t')] \times \cos \left[2 \int_{t'}^t dt'' w_p(t'') \right], \quad (1)$$

³Such simplifications cannot reduce the external field to a plane wave, because in this case the field invariants $\mathcal{F} = (E^2 - B^2)/2$ and $\mathcal{G} = \mathbf{E} \cdot \mathbf{B}$ vanish identically, and the vacuum-vacuum transition amplitude does not decay against electron-positron pairs [42,43].

⁴Hereafter, we assume that the external field is not affected by the process occurring in it. Therefore, we fully disregard the potential realization of avalanche processes [53].

⁵In the following we set the Planck constant equal to unity, $\hbar = 1$.

and in which the vacuum initial condition $W(\mathbf{p}, -\infty) = 0$ is assumed. This equation represents a semiclassical approximation in the sense that the external background field is not quantized while the equation itself results from the quantization of the Dirac field. Note that, hereafter, a dot indicates a total time derivative. We also point out that $W(\mathbf{p}, t)$ involves a sum over both spin states, providing an overall factor 2. The above formula is characterized by the transverse energy squared $\epsilon_{\perp}^2 = m^2 c^4 + \mathbf{p}_{\perp}^2 c^2$ and the total energy squared $w_{\mathbf{p}}^2(t) = \epsilon_{\perp}^2 + [p_{\parallel} - e\mathcal{A}(t)/c]^2 c^2$, with $\mathbf{p}_{\perp} = (p_x, 0, p_z)$ and $\mathbf{p}_{\parallel} = (0, p_y, 0)$ being the components of the canonical momentum perpendicular and parallel to the direction of the field, respectively. Note that the four-potential of the external field $\mathcal{A}_{\mu}(t)$ is chosen in the temporal gauge [$\mathcal{A}_0(t) = 0$] so that $E(t) = -(1/c)d\mathcal{A}/dt$.

Further comments are in order. First, the quantum Vlasov equation [Eq. (1)] does not take into account either the collision between the created particles or their inherent radiation fields. In the presence of a CEF both phenomena are predicted to become relevant as the field strength E reaches the critical scale of QED, $E_c = m^2 c^3 / |e|$ [59,63,65]. So, the solution of Eq. (1) is expected to be trustworthy in the subcritical regime $E \ll E_c$ where the number of produced pairs per unit of volume reads

$$\mathcal{N}_{3+1} = \lim_{t \rightarrow \infty} \int \mathfrak{d}^3 p W(\mathbf{p}, t), \quad (2)$$

with the shorthand notation $\mathfrak{d} \equiv d/(2\pi)$.

Finally, we remark that, when the external field is oscillating in time with frequency ω and amplitude E , the resulting \mathcal{N}_{3+1} should be much smaller than the maximum density $\mathcal{N}_{\max} \sim E^2/(2\omega)$ that can be created from it; otherwise, the external field model is no longer justified.

B. Boltzmann-Vlasov equations in low-dimensional spacetimes

Quantum-kinetic theory constitutes an appropriate approach for investigating the production of electron-positron pairs by a time-dependent electric field in low-dimensional spacetimes. The corresponding quantum Vlasov equations can be derived from the respective Dirac equation in the field by applying a method similar to the one used in the determination of Eq. (1) (for details, we refer the reader to Refs. [56,57]). Alternatively, a dimensional reduction *à la* Kaluza and Klein [66,67] can be carried out on the 3 + 1 quantities, particularly, on the coordinates perpendicular to the field.⁶ By using the latter procedure, we obtain formalisms of different dimensionality.

⁶This requirement is in connection with the 2 + 1-dimensional version of QED in which the electric field lies in the plane defined by the space coordinates.

The first step allows us to describe the production of pairs in a Minkowski space with 2 + 1 dimensions M_{2+1} . In order to show this, we take the dimension in excess x^i to be curled up into a circle S^1 with a radius \mathcal{R} . In this context the motion of the Dirac fermions is confined to the interval $0 \leq x^i \leq 2\pi\mathcal{R}$, and since the compactified coordinate is periodic and the electric field is homogeneous, one can Fourier expand the Dirac field in terms of the corresponding quantized momentum $p_n^i = n\mathcal{R}^{-1}$ with $n \in \mathbb{Z}$. The exponentials involved in this expansion $\sim \exp(inx^i/\mathcal{R})$ heavily oscillate as the limit $\mathcal{R} \rightarrow 0$ is taken into account. In such circumstances, only the fundamental mode $n = 0$, corresponding to vanishing momentum, dominates. Hence, once the momentum \mathbf{p} is locked up to a plane perpendicular to \mathbf{x}^i , the spontaneous production of electron-positron pairs driven by an oscillating electric field (OEF) in a 2 + 1-dimensional spacetime is effectively described by Eq. (1). However, unlike the case in 3 + 1 dimensions, the single-particle distribution function in a 2 + 1-dimensional spacetime does not involve a summation over the double-valued spin indices. We remark that the contribution of this sum is canceled out by dividing the resulting expression for $W(\mathbf{p}, t)$ by a factor 2 [19,45].

It is worth mentioning that the results which follow from this effective description are valid as long as the typical energy involved in the problem is much below the characteristic scale $\epsilon_0 \approx c\mathcal{R}^{-1}$. On the other hand, the expression for the number of produced pairs per unit of area in M_{2+1} results from Eq. (2) by performing a transition to the discrete limit $\int \mathfrak{d}p \rightarrow \frac{1}{2\pi\mathcal{R}} \sum_{p^i}$ in which only the contribution of the vanishing mode must be considered. Accordingly,

$$\mathcal{N}_{2+1} \equiv \frac{1}{2} \lim_{\mathcal{R} \rightarrow 0} 2\pi\mathcal{R} \mathcal{N}_{3+1} = \lim_{t \rightarrow \infty} \int \mathfrak{d}^2 p W_{2+1}(\mathbf{p}, t), \quad (3)$$

where $W_{2+1}(\mathbf{p}, t)$ refers to the single-particle distribution function $W(\mathbf{p}, t)$ divided by 2 and with the momentum component p^i having been set to 0.

Straightforward analyses, similar to those made in the previous case, allow us to apply Eq. (1) when the production of pairs takes place in 1 + 1 dimensions. In such a case, two spatial coordinates have to be compactified on a torus $S^1 \times S^1$, which requires to set the respective components of the quantized momentum to zero as the characteristic radii of this manifold $\tilde{\mathcal{R}}$ and \mathcal{R} vanish identically. Then the asymptotic expression $W_{1+1}(\mathbf{p}, \infty)$, resulting from the quantum Vlasov equation—after dividing by 2—defines the linear density of created particle pairs $\mathcal{N}_{1+1} = \int \mathfrak{d}p W_{1+1}(\mathbf{p}, \infty)$.

We apply the procedure described above by supposing the occurrence of the process in M_{2+1} through a constant electric field [$\mathcal{A}(t) = -cEt$]. Seeking simplicity, we take advantage of the known asymptotic expression for the single-particle distribution function in a four-dimensional spacetime $W(\mathbf{p}, \infty) \approx 2 \exp[-\pi\epsilon_{\perp}^2/(|e|Ec)]$ [45]. After

compactifying the axis lying perpendicular to the external field and considering the fundamental contribution [$p_z = 0$], we find that the rate of PP per unit area is

$$\dot{\mathcal{N}}_{2+1} \approx \frac{(|e|E)^{3/2}}{4\pi^2 c^{1/2}} \exp\left(-\pi \frac{E_c}{E}\right), \quad (4)$$

provided $E \ll E_c$. A similar outcome results in $1 + 1$ dimensions. In this case we obtain that the asymptotic expression of the single-particle distribution function is momentum independent, $W_{1+1}(\infty) \approx \exp[-\pi E_c/E]$, and the rate of yielded particle pairs per unit of length reads

$$\dot{\mathcal{N}}_{1+1} \approx \frac{|e|E}{2\pi} \exp\left(-\pi \frac{E_c}{E}\right). \quad (5)$$

The rates presented in Eqs. (4) and (5) coincide with those previously obtained in Refs. [55,68–70] by other methods. A comparison between both expressions reveals a clear dependence on the respective spacetime topology.

C. Extension to Dirac fermions in graphene layers

We wish to apply the procedure described so far to the production of Dirac fermions in a graphene layer. Since this kind of layer approaches a $2 + 1$ -dimensional system, one could expect that the results previously derived are suited for such a purpose. However, inherent features of this material prevent us from proceeding in a straightforward way. While some of these characteristics can be incorporated, there are other details which require certain attention. For instance, our previous expressions do not take into account effects resulting from finite temperatures. Accordingly, it must be understood that their applicability is trustworthy in the zero temperature limit. Also, we suppose that the electron-hole symmetry is preserved in this layer, a fact theoretically verified within the nearest-neighbors tight-binding model but no longer true as the next-to-nearest-neighbors interactions are considered [27].

In contrast to previous investigations [30,36–38], here and in the following the charge carriers are considered with a tiny mass m corresponding to the gap $\Delta\varepsilon = 2m v_f^2$. In the numerical calculations in Sec. III the specific value $\Delta\varepsilon = 0.26$ eV is chosen for practical purposes; such an energy gap can originate, e.g., from the epitaxial growth of graphene on SiC substrates [39]. For comparison the energy gap $\Delta\varepsilon = 0.12$ eV is considered in addition. We note that other values of the energy gap can also be induced in graphene [40].

Observe that, when adapting the $2 + 1$ -dimensional version of Eq. (1), we have to take into account that—in graphene—the Fermi velocity $v_f \approx c/300$ cannot be exceeded. The inclusion of this constraint demands that one slightly modifies the quantum Boltzmann-Vlasov equations in M_{2+1} , since it characterizes the instability of the vacuum where the created electrons and positrons

might travel with velocities greater than v_f but always smaller than c . Such modifications are carried out by replacing $mc^2 \rightarrow m v_f^2$, $p_i c \rightarrow p_i v_f$, $eEc \rightarrow eE v_f$, $Ac \rightarrow A v_f$ so that the production of quasiparticle-hole pairs in graphene turns out to be governed by

$$\dot{W}_g(\mathbf{p}, t) = Q(\mathbf{p}, t) \int_{-\infty}^t dt' Q(\mathbf{p}, t') \left[\frac{1}{2} - W_g(\mathbf{p}, t') \right] \times \cos \left[2 \int_{t'}^t dt'' w_p(t'') \right], \quad (6)$$

where the function $Q(\mathbf{p}, t) \equiv eE(t)v_f \epsilon_{\perp} / w_p^2(t)$ has been introduced. While $\epsilon_{\perp}^2 = m^2 v_f^4 + p_x^2 v_f^2$ is the transverse energy squared of the Dirac fermions, $w_p^2(t) = \epsilon_{\perp}^2 + [p_y - eA(t)/c]^2 v_f^2$ is their respective total energy squared.

Further comments are in order. First, Eq. (6) shows that the production of electron-hole pairs in graphene is a nonequilibrium phenomenon. Observe that—as in QED—the combination of the nonlocality in time and the memory effects closely associated with the quantum statistic factor $\sim [1/2 - W_g(\mathbf{p}, t)]$ provides Eq. (6) with a pronounced non-Markovian feature [56,59,60]. It means that the single-particle distribution function $W_g(\mathbf{p}, t)$ depends on the number of electron-hole pairs already present in the system. We remark that the spectral information encoded in Eq. (6) will be valid in a vicinity of any of the two inequivalent points in the reciprocal space \mathbf{K}_{\pm} . Accordingly, the momentum of the quasiparticles \mathbf{p} must be understood as relative to \mathbf{K}_{\pm} with $|\mathbf{p}| \ll |\mathbf{K}_{\pm}| = 4\pi/(3\sqrt{3}a_0)$ and $a_0 = 0.142$ nm [24]. It is, indeed, the previous restriction that does guarantee the relativisticlike behavior of the charge carriers. Thus, in calculating the density of pairs per unit of area [Eq. (4)] the respective integral must be carried out over a surface limited by $p_{\max} \ll |\mathbf{K}_{\pm}| \sim 3$ eV/ v_f . As such, the existence of the two inequivalent Dirac points, in combination with the spin degeneracy, leads to four kinds of quasiparticles. Therefore, the total number density of produced particle pairs in graphene is

$$\mathcal{N}_g = 4 \int_{|\mathbf{p}| \ll |\mathbf{K}_{\pm}|} d^2 p W_g(\mathbf{p}, \infty). \quad (7)$$

The application of Eq. (7) to the case driven by a CEF leads to an expression for \mathcal{N}_g that differs from the one which would result from Eq. (4),⁷

$$\mathcal{N}_g \approx \frac{2p_{\max}}{\pi^2} \left(\frac{|e|E}{v_f} \right)^{1/2} \exp\left(-\pi \frac{E_g}{E}\right), \quad (8)$$

⁷The reader interested in the details of this integration may find it helpful to refer to Sec. V of Ref. [36], where it is explained in detail.

where $E_g = m^2 v_f^3 / |e|$ is the critical field in graphene. For example, assuming an energy gap of $\Delta\varepsilon = 0.26$ eV, its value is $E_g \approx 2.6 \times 10^5$ V/cm. It may be seen as arising from the breakdown of the chiral symmetry through the mass m . We note that this critical scale turns out to be much smaller than the critical scale of QED $E_c = 1.3 \times 10^{16}$ V/cm by 11 orders of magnitude. The expression in Eq. (8) can be understood as a ‘‘saturation’’ density of Dirac-like particle pairs in graphene. It is reached when the interaction time with the external CEF approaches $T_{\text{sat}} \sim p_{\text{max}} / (eE)$. For larger interaction times, also particles with momenta exceeding p_{max} are created which are not properly described by the Dirac equation [36,38].

Finally, it must be understood that the effective Boltzmann-Vlasov equations describing the spontaneous creation of electron-hole pairs apply as long as the electric field satisfies the condition $E \ll E_g$. As in the vacuum case, Eq. (6) does not take into account either the effects coming from the inherent radiation of the charge carriers or the collisions between the created quasiparticles.

III. NUMERICAL RESULTS IN AN ELECTRIC FIELD OSCILLATING IN TIME

A. Resonant approach and numerical aspects

The similarity between the kinetic equation describing the PP in graphene [Eq. (6)] and the one corresponding to 3 + 1-dimensional QED [Eq. (1)] allows us to extrapolate various outcomes associated with the production of electron-positron pairs to the graphene scenario. For instance, if the electric field oscillates in time periodically, we expect that $W_g(\mathbf{p}, t)$ resembles the characteristic resonances associated with the absorption of multiple energy packages (‘‘photons’’) from the field [48,54,64,71–73]. This phenomenon takes place as the resonance condition

$$2\bar{\varepsilon}_p \approx n\omega \quad (9)$$

holds. In this relation, n denotes the number of absorbed photons whereas $\bar{\varepsilon}_p = (1/\tau) \int_0^\tau dt w_p(t)$ refers to the quasienergy of the produced particles, i.e., the energy averaged over the total pulse length τ . The behavior of the distribution function $W_{3+1}(\mathbf{p}, t)$ near a resonance characterized by n is also known. Quoting the result derived in [19,54,71] and applying the procedure outlined in the previous section one has that

$$W_{g,n}(\mathbf{p}, t) \approx \frac{1}{4} \frac{|\Lambda_n(\mathbf{p})|^2}{\Omega_{\text{Rabi}}^2(\mathbf{p})} \sin^2[\Omega_{\text{Rabi}}(\mathbf{p})(t - t_{\text{in}})]. \quad (10)$$

The formula above was obtained by supposing that the field is suddenly turned on at t_{in} and instantaneously turned off after the interaction time. Here $\Lambda_n(\mathbf{p})$ is a complex time-independent coefficient whose explicit expression is not

important here. In Eq. (10), $\Omega_{\text{Rabi}}(\mathbf{p}) = \frac{1}{2} [|\Lambda_n(\mathbf{p})|^2 + \Delta_n^2(\mathbf{p})]^{1/2}$ denotes the Rabi-like frequency of the vacuum with $\Delta_n(\mathbf{p}) \equiv 2\bar{\varepsilon}_p - n\omega$ being the detuning parameter. At this point we should mention that the above resonant approximation is valid if the Rabi-like frequency is slow in comparison with the laser frequency, $\Omega_{\text{Rabi}}(\mathbf{p}) \ll \omega$ [72,73].

Let us now investigate the outcome resulting from a numerical evaluation of Eq. (6) when the OEF is described by a potential of the form

$$\mathcal{A}(t) = -\frac{cE}{\omega} \mathcal{F}(\phi) \sin(\phi) \hat{\mathbf{n}}, \quad (11)$$

where ω and E are the frequency and the electric field amplitude, respectively. Besides, here $\phi = \omega t$ and $\hat{\mathbf{n}}^T = (0, 1, 0)$ defines the polarization direction of the field. In Eq. (11) the envelope function is chosen with \sin^2 -shaped turn-on and turn-off segments and a plateau region of constant field intensity in between. Explicitly,

$$\mathcal{F}(\phi) = \begin{cases} \sin^2(\frac{1}{2}\phi) & 0 \leq \phi < \pi \\ 1 & \pi \leq \phi \leq 2\pi\mathcal{K} \\ \sin^2(N\pi - \frac{1}{2}\phi) & 2\pi\mathcal{K} < \phi \leq 2\pi N \\ 0 & \text{otherwise} \end{cases}, \quad (12)$$

where $N = N_{\text{plateau}} + 1$ and $\mathcal{K} = N - \frac{1}{2}$ holds. Observe that Eqs. (11) and (12) guarantee the starting of the OEF with zero amplitude at $t = 0$.

Although Eq. (6) provides various physical insights inherent to the PP process in graphene, its numerical solution is easier to determine when an equivalent system of ordinary differential equations is considered instead,

$$i\dot{f}(\mathbf{p}, t) = a_p(t)f(\mathbf{p}, t) + \ell_p(t)g(\mathbf{p}, t), \quad (13)$$

$$i\dot{g}(\mathbf{p}, t) = \ell_p^*(t)f(\mathbf{p}, t) - a_p(t)g(\mathbf{p}, t). \quad (14)$$

In this context the distribution function is given by $W_g(\mathbf{p}, t) = |f(\mathbf{p}, t)|^2$ and the initial conditions are chosen so that $f(\mathbf{p}, -\infty) = 0$ and $g(\mathbf{p}, -\infty) = 1$. The remaining parameters contained in these formulas are given by

$$a_p(t) = w_p(t) + \frac{eE(t)p_x v_f^2}{2w_p(t)[w_p(t) + m v_f^2]},$$

$$\ell_p(t) = \frac{1}{2} \frac{eE(t)v_f \epsilon_\perp}{w_p^2(t)} \exp \left[-i \arctan \left(\frac{p_x q_{\parallel} v_f^2}{\epsilon_\perp^2 + m v_f^2 w_p(t)} \right) \right],$$

where the longitudinal kinetic momentum is $q_{\parallel} = p_y - e\mathcal{A}(t)/c$. The equivalence between Eq. (6) and the system above [Eqs. (13) and (14)] has been mathematically established in several references (see for instance [19,45,56]). However, it is worth mentioning that various

representations of the Boltzmann-Vlasov equation can be found in the literature. Their use is mainly motivated by an optimization of the numeric assessment.

B. Results and discussions

As mentioned in the previous section, the mass of the Dirac fermions is taken as $m = \Delta\varepsilon/2v_f^2$, which corresponds to $m \approx 5.4$ keV/ c^2 for $\Delta\varepsilon = 0.12$ eV and $m \approx 11.7$ keV/ c^2 for $\Delta\varepsilon = 0.26$ eV. We set the field frequency to $\omega = 24.032$ meV. The plateau region comprises $N_{\text{plateau}} = 241$ cycles so that the total pulse length is $\tau = 2\pi N/\omega \approx 41.625$ ps. On the other hand, the field strength is taken as $E = 6.6 \times 10^4$ V/cm, which corresponds to a peak laser intensity $I = cE^2 \approx 1.1 \times 10^7$ W/cm 2 . This particular set of parameters has been chosen in such a way that, for the massive model with $\Delta\varepsilon = 0.26$ eV, the single-particle distribution function $W_g(\mathbf{0}, t)$ hits a resonance corresponding to the absorption of $n \approx 15$ photons from the strong OEF [see Eq. (9)]. At this point, we remark that similar field parameters are comfortably attainable with terahertz laser pulses of picosecond duration [74,75]. Likewise, the presence of a critical field E_g establishes a typical scale of intensity in graphene $I_g = cE_g^2$ which amounts to $I_g \approx 1.8 \times 10^8$ W/cm 2 for $\Delta\varepsilon = 0.26$ eV. This intensity level can be easily approached and overpassed with the current laser technology.

The system of differential equations [Eqs. (13) and (14)] has been solved varying the momentum components in the range -0.4 eV $\leq p_{x,y}v_f \leq 0.4$ eV. The results of this assessment are displayed in Fig. 1 in a density color scheme which corresponds to $\log_{10}[W_g(\mathbf{p}, \tau)]$. While the upper panel shows for comparison the outcomes associated with a massless model [$m = 0$], the effects coming from the chiral symmetry breaking are displayed in the lower one. Manifestly, the spectral density associated with massive particles looks different as compared with the model of massless carriers. For instance, at zero momenta [$\mathbf{p} = 0$], the distribution function associated with massive carriers reaches the maximum value [$W_g(0, \tau) = 1$], whereas the corresponding result for the massless model is minimum [$W_g(0, \tau) = 0$]. This minimal value extends along the vertical line located at $p_x = 0$, which constitutes an inherent feature of this scenario. Its occurrence can be anticipated already in Eq. (6) by noting that its right-hand side is proportional to the transverse energy squared [$\varepsilon_{\perp}^2 = p_x^2 v_f^2 + m^2 v_f^4$], which vanishes identically when the carriers are massless and $p_x \rightarrow 0$. In such a situation, the kinetic equation reduces to $\dot{W}_g(p_y, t) = 0$ and the only conceivable solution—in accordance with our initial condition—is $W_g(p_y, t) = 0$.

The ringlike structures displayed in each panel are understood as isocontours of quasienergy $\tilde{\varepsilon}_p$ satisfying the resonance condition [Eq. (9)] and, accordingly, the

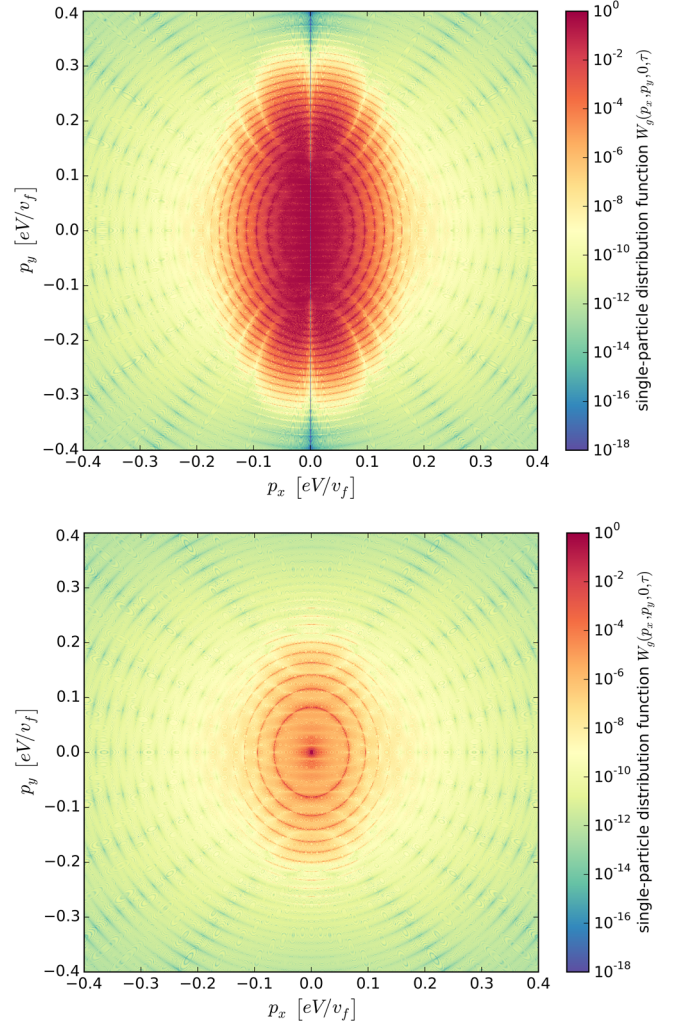


FIG. 1. Logarithmic plots of the single-particle distribution functions for models involving massless (upper panel) and massive ($\Delta\varepsilon = 0.26$ eV, lower panel) charged carriers are displayed. In both cases the external parameters were chosen as follows: $E = 6.6 \times 10^4$ V/cm, $\tau \approx 41.625$ ps and $\omega = 24.032$ meV.

number of photons involved in each resonant process can be inferred. So, further insights on $W_g(\mathbf{p}, \tau)$ can be acquired by contrasting the numerical results with the approached behavior near a resonance [Eq. (10)]. To this end, $W_{g,n}(\mathbf{p}, t)$ is evaluated for times larger than the interaction time [$t > \tau$], when it has become constant. At the resonance, i.e., where Eq. (9) holds [$\Delta_n \approx 0$], the Rabi-like frequency reduces to $\Omega_{\text{Rabi}}(\mathbf{p}) \approx \frac{1}{2}|\Lambda_n(\mathbf{p})|$ and

$$W_{g,n}(\mathbf{p}, \infty) \approx \sin^2[\Omega_{\text{Rabi}}(\mathbf{p})\tau]. \quad (15)$$

For a given interacting time τ , Eq. (15) achieves its maximum value [$W_{g,n}(\mathbf{p}_0, t) = 1$] for a certain momenta combination $\mathbf{p}_0 = (p_{x0}, p_{y0})$ provided $\Omega_{\text{Rabi}}(\mathbf{p}_0) = (2k + 1)\pi/(2\tau)$ with $k \in \mathbb{Z}$ being satisfied. Clearly, our previous discussion indicates that the former has been

chosen so that the maximum is achieved at $\mathbf{p} = 0$. Observe that, away from the resonance, i.e., for $\Delta_n \neq 0$, the amplitude of $W_{g,n}(\mathbf{p}, \tau)$ decreases [see Eq. (10)]. This trend manifests in both panels around each resonance in the form of light red—sometimes orange—valleys. Additionally, they reveal a gradual decrement in the single-particle distribution functions as the momentum components increase.

We note that the isocontours resemble ellipses with the major axis lying along the longitudinal direction. The elongation along the p_y axis is an outcome of the asymmetry introduced by the external field in Eq. (6) through the term $p_y - eA(t)/c$, and indicates that the creation of a particle (hole, respectively) with rather large longitudinal momentum is more likely to take place than with a correspondingly large transverse momentum. Such a trend resembles the pattern occurring in a CEF, where the distribution function is homogeneous along the longitudinal direction but suppressed by a Gaussian profile transversally. Furthermore, a comparison between both panels reveals that the red-colored region in the massless model is considerably larger than the corresponding region for the massive scenario, where only a few resonances arise. This indicates that the volume below the surface $W_g(p_x, p_y)$ for the former exceeds the one associated with the cases driven by massive carriers. Since both volumes result from the integration over the momentum components, actually they determine the number of pairs yielded for each scenario in a vicinity of a Dirac point. Hence, the results shown in Fig. 1 already provide evidence that the density of created pairs in the massless case is substantially larger than the one resulting from the situation dealing with massive carriers.

The previous claim is verified in Fig. 2, where the behavior of Eq. (7) with respect to the electric field strength E is shown. In this figure, the green curve describes the number of pairs yielded per cm^2 for massless charges, whereas the one in blue corresponds to the massive carrier model with $\Delta\varepsilon = 0.26$ eV. For comparison, the respective outcomes in a CEF have been included. Figure 2 shows that the production efficiency for the case of massive particles is strongly reduced by several orders of magnitude. This mainly reflects the impact of the Schwinger-like exponential factor in Eq. (8) which is absent when the particles are massless. Accordingly, the curves for the massless case are rather flat, whereas the curves for massive Dirac fermions exhibit a much stronger dependence on the applied electric field strength.

For the case of massive particles with $\Delta\varepsilon = 0.26$ eV, our numerical results for an OEF and the analytical prediction for a CEF lie quite close to each other at field strengths above $E \gtrsim 4 \times 10^4$ V/cm. This may be understood by observing that the field oscillations are rather slow [$\omega \ll m$] such that the OEF locally resembles a CEF. Besides, the dimensionless intensity parameter $\xi_g = |e|E/(m\omega v_f)$ is of order unity here ($\xi_g = 1$ corresponds

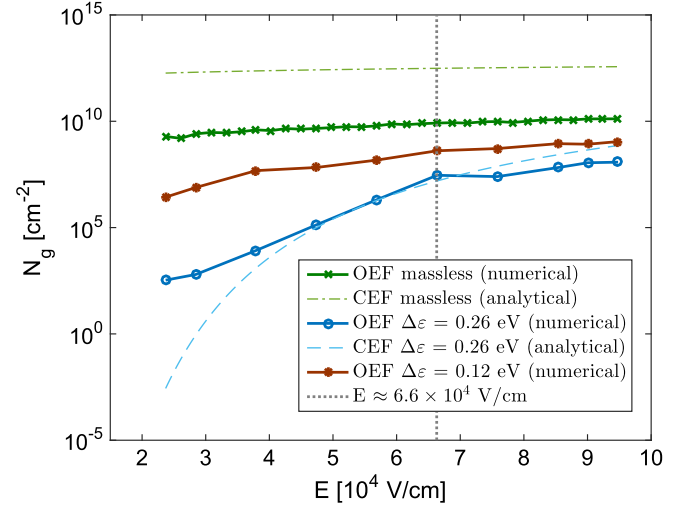


FIG. 2. Number of electron-hole pairs produced per cm^2 in an OEF. While the result for massless carriers is in green, the outcome for massive charges is shown in red and blue, with the data points connected by straight lines. Also, for comparison, the curves corresponding to the cases driven by a CEF [see Eq. (8)] are displayed in a green dash-dotted line (for massless) and blue dashed line (for massive). Here the vertical grey dashed line indicates the electric field value which was used in Fig. 1. The same benchmark values and notation of Fig. 1 must be understood.

to $E \approx 4.7 \times 10^4$ V/cm for the gap value chosen, $\Delta\varepsilon = 0.26$ eV). Contrary to that, for smaller field strengths below $E \lesssim 3 \times 10^4$ V/cm, the pair density produced by an OEF is significantly larger than the CEF outcome. The reason is that in an OEF pairs can be generated both by the field amplitude but also by the time dependence of the field [37,38]; the latter channel is absent in a CEF. Accordingly, for $\xi_g < 1$, the creation mechanism by multiphoton absorption can become dominant, leading to enhanced pair creation in an OEF as compared with a CEF.

For the case of massless particles, our numerical results for an OEF and the analytical prediction for a CEF in Fig. 2 run almost parallel. However, the CEF outcome—which describes the saturation density in accordance with Eq. (8)—is larger by a few orders of magnitude. We argue that this is because the field oscillations can be considered as very fast in this case [$\omega \gg m = 0$]. Hence, the effective field strength acting during the pair formation time is reduced by a corresponding temporal average, leading to the strong suppression observed in Fig. 2. We point out that this behavior is different in a nonoscillating, Sauter-like electric field whose pair creation efficiency of massless charge carriers in graphene approaches the CEF result to within a factor of order unity [36].

For comparison, Fig. 2 also shows our estimates for the number of massive pairs produced in graphene with a reduced gap of $\Delta\varepsilon = 0.12$ eV. As one might have expected, the number is significantly larger than in the case of $\Delta\varepsilon = 0.26$ eV and approaches the massless limit.

We note that the critical field in the case presently under consideration only amounts to $E_g \simeq 5.5 \times 10^4$ V/cm. Since this turns out to be comparable with the values encompassed in the picture, the analytical expression associated with a constant electric field does not apply and the corresponding curve is not shown here.

IV. CONCLUSION AND OUTLOOK

In summary, we have started by presenting the fundamental aspects associated with the production of pairs in a 3 + 1-dimensional spacetime for the specific case in which the external gauge potential is independent of the space coordinates but oscillates in time. With the aim of investigating PP in low-dimensional Minkowski spaces, dimensional compactifications have been carried out. The resulting effective theories verify that the production process in 2 + 1- and 1 + 1-dimensional spacetime is appropriately described by quantum-kinetic Boltzmann-Vlasov equations.

We have applied the former outcome to the production of massive Dirac fermions in graphene layers. The situation driven by an electric field oscillating in time has been investigated, which is characterized by a pronounced resonant behavior. The latter is reflected in the momentum distribution of created pairs. The total number density of massive pairs shows a strong dependence on the applied electric field strength which is mainly due to the Schwinger-like exponential factor involving the critical

field amplitude in graphene. Its occurrence is an important consequence of the massive quasiparticles in bandgap graphene layers, as compared with the massless charge carriers in ordinary gap-free graphene. Differences between the pair densities obtained in oscillating and constant electric fields, respectively, could be traced back to the impact of the field oscillations.

Our numerical findings have shown that terahertz laser pulses—in combination with the substrate-induced bandgap technique for graphene—might provide a feasible scenario in which the creation of light quasiparticle-hole pairs could take place, in this way simulating the vacuum instability in QED. In connection, it remains an open question whether the production rate of massless quasiparticles in a single mode field can be comparable to the results associated with light massive Dirac fermions when a weak beam of energetic photons is superimposed onto a strong but low-frequency electric field. We plan to present a detailed investigation of this subject in a forthcoming publication.

ACKNOWLEDGMENTS

We thank Thomas Heinzl, Alexander B. Voitkiv, and Hengyi Xu for useful discussions. S. V. gratefully acknowledges the support of the Alexander von Humboldt Foundation in the early stage of this project. R. E. acknowledges funding by the network SPP Grant No. 1459 of the German Research Foundation (DFG).

-
- [1] F. Sauter, Über das Verhalten eines Elektrons im homogenen elektrischen Feld nach der relativistischen Theorie Diracs, *Z. Phys.* **69**, 742 (1931).
 - [2] W. Heisenberg and H. Euler, Consequences of Dirac's theory of positron, *Z. Phys.* **98**, 714 (1936).
 - [3] J. S. Schwinger, On gauge invariance and vacuum polarization, *Phys. Rev.* **82**, 664 (1951).
 - [4] A. Casher, H. Neuberger, and S. Nussinov, Chromoelectric flux tube model of particle production, *Phys. Rev. D* **20**, 179 (1979).
 - [5] J. Rafelski, L. P. Fulcher, and A. Klein, Fermions and bosons interacting with arbitrarily strong external fields, *Phys. Rep.* **38**, 227 (1978).
 - [6] M. Kachelriess, Neutrino self-energy and pair creation in neutron stars, *Phys. Lett. B* **426**, 89 (1998).
 - [7] D. Kharzeev, E. Levin, and K. Tuchin, Multiparticle production and thermalization in high-energy QCD, *Phys. Rev. C* **75**, 044903 (2007).
 - [8] See the website of the Extreme Light Infrastructure available at: <http://www.eli-laser.eu/>.
 - [9] See the website of the Exawatt Center for Extreme Light Studies available at: <http://www.xcels.iapras.ru/>.
 - [10] S. S. Bulanov, V. D. Mur, N. B. Narozhny, J. Nees, and V. S. Popov, Multiple Colliding Electromagnetic Pulses: A Way to Lower the Threshold of e^+e^- Pair Production from Vacuum, *Phys. Rev. Lett.* **104**, 220404 (2010).
 - [11] D. L. Burke *et al.*, Positron Production in Multiphoton Light-by-Light Scattering, *Phys. Rev. Lett.* **79**, 1626 (1997).
 - [12] C. Müller, A. B. Voitkiv, and N. Grün, Differential rates for multiphoton pair production by an ultrarelativistic nucleus colliding with an intense laser beam, *Phys. Rev. A* **67**, 063407 (2003).
 - [13] P. Sieczka, K. Krajewska, J. Z. Kamiński, P. Panek, and F. Ehlotzky, Electron-positron pair creation by powerful laser-ion impact, *Phys. Rev. A* **73**, 053409 (2006).
 - [14] G. V. Dunne, H. Gies, and R. Schützhold, Catalysis of Schwinger vacuum pair production, *Phys. Rev. D* **80**, 111301 (2009).
 - [15] A. Di Piazza, E. Lötstedt, A. I. Milstein, and C. H. Keitel, Barrier Control in Tunneling e^+e^- Photoproduction, *Phys. Rev. Lett.* **103**, 170403 (2009).
 - [16] M. Orthaber, F. Hebenstreit, and R. Alkofer, Momentum spectra for dynamically assisted Schwinger pair production, *Phys. Lett. B* **698**, 80 (2011).

- [17] M. Jiang, W. Su, Z. Q. Lv, X. Lu, Y. J. Li, R. Grobe, and Q. Su, Pair creation enhancement due to combined external fields, *Phys. Rev. A* **85**, 033408 (2012).
- [18] M. J. A. Jansen and C. Müller, Strongly enhanced pair production in combined high- and low-frequency laser fields, *Phys. Rev. A* **88**, 052125 (2013).
- [19] I. Akal, S. Villalba-Chávez, and C. Müller, Electron-positron pair production in a bifrequent oscillating electric field, *Phys. Rev. D* **90**, 113004 (2014).
- [20] A. Otto, D. Seipt, D. Blaschke, B. Kämpfer, and S. A. Smolyansky, Lifting shell structures in the dynamically assisted Schwinger effect in periodic fields, *Phys. Lett. B* **740**, 335 (2015).
- [21] K. S. Novoselov *et al.*, Electric field effect in atomically thin carbon films, *Science* **306**, 666 (2004).
- [22] K. S. Novoselov, D. Jiang, F. Schedin, T. J. Booth, V. V. Khotkevich, S. V. Morozov, and A. K. Geim, Two-dimensional atomic crystals, *Proc. Natl. Acad. Sci. U.S.A.* **102**, 10451 (2005).
- [23] K. S. Novoselov, A. K. Geim, S. V. Morozov, D. Jiang, M. I. Katsnelson, I. V. Grigorieva, S. V. Dubonos, and A. A. Firsov, Two-dimensional gas of massless Dirac fermions in graphene, *Nature (London)* **438**, 197 (2005).
- [24] A. H. Castro Neto, F. Guinea, N. M. R. Peres, K. S. Novoselov, and A. K. Geim, The electronic properties of graphene, *Rev. Mod. Phys.* **81**, 109 (2009).
- [25] V. N. Kotov, B. U. Uchoa, V. M. Pereira, F. Guinea, and A. H. Castro Neto, Electron-electron interactions in graphene: Current status and perspectives, *Rev. Mod. Phys.* **84**, 1067 (2012).
- [26] D. N. Basov, M. M. Fogler, A. Lanzara, F. Wang, and Y. Zhang, Colloquium: Graphene spectroscopy, *Rev. Mod. Phys.* **86**, 959 (2014).
- [27] P. R. Wallace, The band theory of graphite, *Phys. Rev.* **71**, 622 (1947).
- [28] M. I. Katsnelson, K. S. Novoselov, and A. K. Geim, Chiral tunneling and the Klein paradox in graphene, *Nat. Phys.* **2**, 620 (2006).
- [29] A. De Martino, D. Klöpfer, D. Matrasulov, and R. Egger, Electric-Dipole-Induced Universality for Dirac Fermions in Graphene, *Phys. Rev. Lett.* **112**, 186603 (2014).
- [30] D. Allor, T. D. Cohen, and D. A. McGady, The Schwinger mechanism and graphene, *Phys. Rev. D* **78**, 096009 (2008).
- [31] M. Lewkowicz and B. Rosenstein, Dynamics of Particle-Hole Pair Creation in Graphene, *Phys. Rev. Lett.* **102**, 106802 (2009).
- [32] M. Lewkowicz, H. C. Kao, and B. Rosenstein, Signature of the Schwinger pair creation rate via radiation generated in graphene by a strong electric current, *Phys. Rev. B* **84**, 035414 (2011).
- [33] N. Yokomizo, Radiation from electrons in graphene in strong electric field, *Ann. Phys. (New York)* **351**, 166 (2014).
- [34] B. Dora and R. Moessner, Nonlinear electric transport in graphene: quantum quench dynamics and the Schwinger mechanism, *Phys. Rev. B* **81**, 165431 (2010).
- [35] B. Dora and R. Moessner, Dynamics of the spin Hall effect in topological insulators and graphene, *Phys. Rev. B* **83**, 073403 (2011).
- [36] G. L. Klimchitskaya and V. M. Mostepanenko, Creation of quasiparticles in graphene by a time-dependent electric field, *Phys. Rev. D* **87**, 125011 (2013).
- [37] H. K. Avetissian, A. K. Avetissian, G. F. Mkrtchian, and Kh. V. Sedrakian, Creation of particle-hole superposition states in graphene at multiphoton resonant excitation by laser radiation, *Phys. Rev. B* **85**, 115443 (2012).
- [38] F. Fillion-Gourdeau and S. MacLean, Time-dependent pair creation and the Schwinger mechanism in graphene, *Phys. Rev. B* **92**, 035401 (2015).
- [39] S. Y. Zhou, G.-H. Gweon, A. V. Fedorov, P. N. First, W. A. de Heer, D.-H. Lee, F. Guinea, A. H. Castro Neto, and A. Lanzara, Substrate-induced bandgap opening in epitaxial graphene, *Nat. Mater.* **6**, 770 (2007).
- [40] G. Giovannetti, P. A. Khomyakov, G. Brocks, P. J. Kelly, and J. van den Brink, Substrate-induced band gap in graphene on hexagonal boron nitride: ab initio density functional calculations, *Phys. Rev. B* **76**, 073103 (2007).
- [41] A. Varykhalov, J. Sánchez-Barriga, A. M. Shikin, C. Biswas, E. Vescovo, A. Rybkin, D. Marchenko, and O. Rader, Electronic and Magnetic Properties of Quasifree-standing Graphene on Ni, *Phys. Rev. Lett.* **101**, 157601 (2008).
- [42] E. S. Fradkin, D. M. Gitman, and S. M. Shvartsman, *Quantum Electrodynamics with Unstable Vacuum* (Springer-Verlag, Berlin, 1991).
- [43] G. V. Dunne, in *From Fields to Strings*, edited by M. Shifman *et al.* (World Scientific, Singapore, 2005), Vol. 1, pp. 445–522.
- [44] M. Ruf, G. R. Mocken, C. Müller, K. Z. Hatsagortsyan, and C. H. Keitel, Pair Production in Laser Fields Oscillating in Space and Time, *Phys. Rev. Lett.* **102**, 080402 (2009).
- [45] F. Hebenstreit, R. Alkofer, and H. Gies, Schwinger pair production in space- and time-dependent electric fields: relating the Wigner formalism to quantum-kinetic theory, *Phys. Rev. D* **82**, 105026 (2010).
- [46] A. A. Grib, V. M. Mostepanenko, and V. M. Frolov, Particle creation from vacuum by the homogeneous electric field in canonical formalism, *Theor. Math. Phys.* **13**, 1207 (1972).
- [47] A. I. Nikishov, Pair production by a constant external field, *Sov. Phys. JETP* **30**, 660 (1970).
- [48] V. S. Popov, Resonant pair production in a strong electric field, *JETP Lett.* **18**, 255 (1973).
- [49] E. Brezin and C. Itzykson, Pair production in vacuum by an alternating field, *Phys. Rev. D* **2**, 1191 (1970).
- [50] V. G. Bagrov, D. M. Gitman, and Sh. M. Shvartsman, Concerning the production of electron-positron pairs from vacuum, *Sov. Phys. JETP* **41**, 191 (1975).
- [51] D. M. Gitman, Processes of arbitrary order in quantum electrodynamics with a pair-creating external field, *J. Phys. A* **10**, 2007 (1977).
- [52] Y. I. Salamin, S. Hu, K. Z. Hatsagortsyan, and C. H. Keitel, Relativistic high-power laser-matter interactions, *Phys. Rep.* **427**, 41 (2006).
- [53] A. M. Fedotov, N. B. Narozhny, G. Mourou, and G. Korn, Limitations on the Attainable Intensity of High Power Lasers, *Phys. Rev. Lett.* **105**, 080402 (2010).
- [54] N. B. Narozhnyi and A. I. Nikishov, Pair production by a periodic electric field, *Sov. Phys. JETP* **38**, 427 (1974).
- [55] S. P. Gavrilov and D. M. Gitman, Vacuum instability in external fields, *Phys. Rev. D* **53**, 7162 (1996).

- [56] S. M. Schmidt, D. Blaschke, G. Röpke, S. A. Smolyansky, and A. V. Prozorkevich, A quantum-kinetic equation for particle production in the Schwinger mechanism, *Int. J. Mod. Phys. E* **7**, 709 (1998).
- [57] S. M. Schmidt, D. Blaschke, G. Röpke, A. V. Prozorkevich, S. A. Smolyansky, and V. D. Toneev, Non-Markovian effects in strong-field pair creation, *Phys. Rev. D* **59**, 094005 (1999).
- [58] R. Alkofer, M. B. Hecht, C. D. Roberts, S. M. Schmidt, and D. V. Vinnik, Pair Creation and an X-Ray Free Electron Laser, *Phys. Rev. Lett.* **87**, 193902 (2001).
- [59] J. C. R. Bloch, V. A. Mizerny, A. V. Prozorkevich, C. D. Roberts, S. M. Schmidt, S. A. Smolyansky, and D. V. Vinnik, Pair creation: backreactions and damping, *Phys. Rev. D* **60**, 116011 (1999).
- [60] D. V. Vinnik, R. Alkofer, S. M. Schmidt, S. A. Smolyansky, V. V. Skokov, and A. V. Prozorkevich, Coupled fermion and boson production in a strong background mean field, *Few-Body Syst.* **32**, 23 (2002).
- [61] F. Hebenstreit, R. Alkofer, G. Dunne, and H. Gies, Momentum Signatures for Schwinger Pair Production in Short Laser Pulses with Subcycle Structure, *Phys. Rev. Lett.* **102**, 150404 (2009).
- [62] C. Kohlfürst, M. Mitter, G. von Winckel, F. Hebenstreit, and R. Alkofer, Optimizing the pulse shape for Schwinger pair production, *Phys. Rev. D* **88**, 045028 (2013).
- [63] D. V. Vinnik, A. V. Prozorkevich, S. A. Smolyansky, V. D. Toneev, C. D. Roberts, and S. M. Schmidt, Plasma production and thermalization in a strong field, *Eur. Phys. J. C* **22**, 341 (2001).
- [64] D. B. Blaschke, B. Kämpfer, A. D. Panferov, A. V. Prozorkevich, and S. A. Smolyansky, Influence of laser pulse parameters on the properties of e^-e^+ plasma created from vacuum, *Contrib. Plasma Phys.* **53**, 165 (2013).
- [65] N. Tanji, Dynamical view of pair creation in uniform electric and magnetic fields, *Ann. Phys. (Amsterdam)* **324**, 1691 (2009).
- [66] T. Kaluza, On the problem of unity in physics, *Sitzungsber. Preuss. Akad. Wiss. Berlin (Math. Phys.)* **1921**, 966 (1921).
- [67] O. Klein, Quantum theory and five-dimensional theory of relativity, *Z. Phys.* **37**, 895 (1926).
- [68] S. P. Kim and D. N. Page, Schwinger pair production via instantons in a strong electric field, *Phys. Rev. D* **65**, 105002 (2002).
- [69] T. D. Cohen and D. A. McGady, The Schwinger mechanism revisited, *Phys. Rev. D* **78**, 036008 (2008).
- [70] F. Hebenstreit, J. Berges, and D. Gelfand, Simulating fermion production in 1 + 1 dimensional QED, *Phys. Rev. D* **87**, 105006 (2013).
- [71] V. M. Mostepanenko and V. M. Frolov, Particle creation from vacuum by homogeneous electric field with a periodical time dependence, *Sov. J. Nucl. Phys.* **19**, 451 (1974).
- [72] H. K. Avetissian, A. K. Avetissian, G. F. Mkrtchian, and Kh. Sedrakian, Electron-positron pair production in the field of superstrong oppositely directed laser beams, *Phys. Rev. E* **66**, 016502 (2002).
- [73] G. R. Mocken, M. Ruf, C. Müller, and C. H. Keitel, Nonperturbative multiphoton electron-positron-pair creation in laser fields, *Phys. Rev. A* **81**, 022122 (2010).
- [74] D. J. Cook and R. M. Hochstrasser, Intense terahertz pulses by four-wave rectification in air, *Opt. Lett.* **25**, 1210 (2000).
- [75] T. Bartel, P. Gaal, K. Reimann, M. Woerner, and T. Elsaesser, Generation of single-cycle THz transients with high electric-field amplitudes, *Opt. Lett.* **30**, 2805 (2005).